18th Australasian Fluid Mechanics Conference
Launceston, Australia
3-7 December 2012

Comparison of the Rayleigh–Plesset and Gilmore Equations and Additional Aspects for the Modelling of Seismic Airgun Bubble Dynamics

K. L. de Graaf, I. Penesis and P. A. Brandner

Australian Maritime College
University of Tasmania, Tasmania, 7250, Australia

Abstract

Seismic airguns are commonly used in geophysical exploration. More recently, they are also being used as an alternative to underwater explosions for the shock testing of defence vessels. The study of the dynamics of the bubble produced by a seismic airgun is beneficial in understanding the resultant pressure field and shockwave.

The Rayleigh–Plesset and Gilmore equations for modelling spherical bubble dynamics are compared for the expansion of an initially highly pressurised gas bubble. The relationship between initial gas pressure and both the first maximum bubble radius and the first period of oscillation are presented. The initial gas pressure is non-dimensionalised against hydrostatic pressure and studied over a range of 1 – 50. The separate contributions of presence of the airgun body, mass throttling, effective viscosity and heat diffusion to the first maximum radius and period are modelled and discussed. The effects of evaporation and condensation at the bubble wall are also considered.

Introduction

The Royal Australian Navy is currently investigating the feasibility and advantages of employing seismic airguns for shock testing naval craft. Shock testing with seismic airguns, rather than high explosives, is less expensive, safer, and more environmentally friendly. To perform shock testing effectively, an array of airguns must be used and the interactions between the bubbles can alter the pressure fields produced. Several methods exist for calculating the interactions between bubbles in an array [9, 14], but all rely on a basic understanding of the parameters affecting a single airgun bubble and the pressure field and shockwave produced.

The Gilmore equation for bubble dynamics is commonly used as the underlying basis for seismic airgun bubbles and underwater explosions. Comparisons exist of this equation with other bubble models, including the well known Rayleigh–Plesset equation; however, they consider a bubble's collapse from its maximum radius rather than expansion from its minimum radius. In modelling seismic airgun bubbles it is more practical to consider the initial bubble pressure and radius, rather than the conditions at the first maximum. The present work compares the Gilmore equation to the Rayleigh–Plesset equation to confirm the use of the Gilmore equation as the basic bubble model.

Several contributions have been made to improve the numerical modelling of individual seismic airgun bubbles by considering additional factors to the basic bubble dynamics. Ziolkowski [17] used Gilmore's equation and found a polytropic index of 1.13 gave good results for the first period of oscillation; this value was also obtained by Dragoset [2] for a range of gun sizes. Shulze–Gatterman [13] emphasised the effect of the actual airgun body on the period of oscillation. Safar [12] compared the equation of a bubble to an electrical circuit and developed a model for the rise time, amplitude of the initial pulse, and period of the airgun. Johnston [7] and Dragoset [2] considered the effect of the shuttle motion and choked flow rate on the chamber pressure, with Dragoset allowing for the actual port size. Ziolkowski [18] proposed that heat transfer occurs through the latent heat released by evaporation and condensation at the bubble wall. This concept is repeated by Langhammer and Landro [8]. Laws et al. [9] consider mass transfer due to evaporation and condensation, classical heat diffusion, flow throttling and an 'effective viscosity' induced by the turbulent nature of the bubble. It is claimed that this turbulent nature also has an amplifying effect on the heat transfer across the bubble wall. Li et al [10] includes the effect of mass throttling (but not choked flow) through ports, the airgun body, heat transfer and hydrostatic pressure changes as the bubble rises through the water.

There appears to be no work that considers all of these parameters together and provides values for coefficients with a summary of the impact of each parameter on the bubble behaviour. The present work uses the Gilmore equation as the basic bubble model and considers the individual effects of the presence of the airgun body, mass throttling, effective viscosity, heat diffusion and condensation and evaporation, providing a summary of each contribution.

Comparison of Rayleigh–Plesset and Gilmore Equations

The Rayleigh–Plesset equation describes the motion of a spherical bubble in an incompressible liquid [3]. When considering bubble velocities of an appreciable order of magnitude compared with the speed of sound in water, compressibility of the liquid cannot be ignored. The Gilmore equation includes second-order compressibility terms, accounting for the loss of bubble energy due to the radiated pressure waves [5]. Both equations are commonly used to model bubble dynamics, with the Gilmore equation often used in underwater explosion applications. The Rayleigh–Plesset equation is given by:

$$\rho\left[R\ddot{R}+\frac{3}{2}\dot{R}^2\right]=p_0\left(\frac{R_0}{R}\right)^{3k}+p_v-\frac{2S}{R}-4\mu\frac{\dot{R}}{R}-p_\infty(t) \quad (1)$$

The Gilmore equation is given by:

$$R\ddot{R}\left(1+\frac{\dot{R}}{c}\right)+\frac{3}{2}\dot{R}^2\left(1-\frac{\dot{R}}{3c}\right)=H\left(1+\frac{\dot{R}}{c}\right)\dot{H} \quad (2)$$

where

$$H=n\left(\frac{p_\infty+B}{(n-1)\rho}\right)\left[\left(\frac{p+B}{p_\infty+B}\right)^{\frac{n-1}{n}}-1\right] \quad (3)$$

$$c=c_\infty\left[\left(\frac{p+B}{p_\infty+B}\right)^{\frac{n-1}{2n}}\right] \quad (4)$$

$$p=p_0\left(\frac{R_0}{R}\right)^{3k}+p_v-\frac{2S}{R}-4\mu\frac{\dot{R}}{R} \quad (5)$$

$$c_\infty=\sqrt{n\left(\frac{p_\infty+B}{\rho}\right)} \quad (6)$$

R is the bubble radius, ρ is the water density, p_v is the vapour pressure, p_∞ is the hydrostatic pressure, p_0 is the initial non-condensable gas pressure, R_0 is the initial bubble radius, k is the polytropic index, which varies between 1 (isothermal) and 1.4 (adiabatic) — taken as 1.4 in this work where required, S is the surface tension, μ is the dynamic viscosity, H is the enthalpy difference between the liquid at pressure p and p_∞, and c_∞ is the speed of sound in water at an infinite distance from the bubble. B and n are constants used to calculate the local speed of sound, c, and enthalpy. Gilmore [5] gives B = 3000 atm and n = 7. Overdots represent differentiation with respect to time.

Vokurka [15] compared these two equations for bubble collapse and determined that for amplitudes $(R_{max}/R_{equilibrium})$ greater than 2, the Gilmore equation produces superior results. The first maximum radius as a function of the initial pressure for expanding bubbles is shown in figure 1. The maximum radius is non-dimensionalised with respect to the initial radius and the initial pressure with respect to the hydrostatic water pressure. The results start to diverge for pressure ratios greater than about 3. The Gilmore equation is considered to produce the more accurate results due to the presence of the higher order terms. In

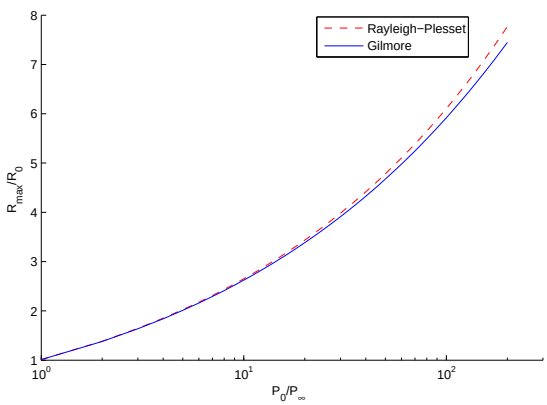

Figure 1: First maximum radius as a function of initial pressure predicted by Rayleigh–Plesset and Gilmore equations.

the study of bubble collapses, the collapse of a Gilmore bubble is fractionally (1.005) [3] longer than the collapse of a Rayleigh bubble. When modelling the bubble expansion and collapse, it is found that a Gilmore bubble has a shorter period than the Rayleigh bubble because a smaller maximum amplitude is predicted (figure 2). Due to the size of the airgun bubbles modelled, it is also found that the surface tension and dynamic viscosity terms are negligible in both solutions. For seismic airguns, the initial pressure is generally at least an order of magnitude greater than the hydrostatic pressure; therefore, while this study is interesting, the overlap between the Rayleigh–Plesset and Gilmore equations is insignificant in the study of airguns. As the Gilmore equation is considered more accurate, all further predictions will use this as the base model. The surface tension term will be ignored. Dynamic viscosity is taken as 1×10^{-3} kg/ms as it is required when calculating the effective viscosity and the thermal boundary layer.

Additional Aspects to the Gilmore Equation

It is well noted [9, 13, 18, 10] that while the Gilmore equation models compressibility which leads to acoustic damping, additional damping parameters must also be present in the dynamics of an airgun bubble. Typically, a real airgun bubble will have lost its energy after only a few growth/collapse cycles. Predictions with the Gilmore equation result in oscillations that persist

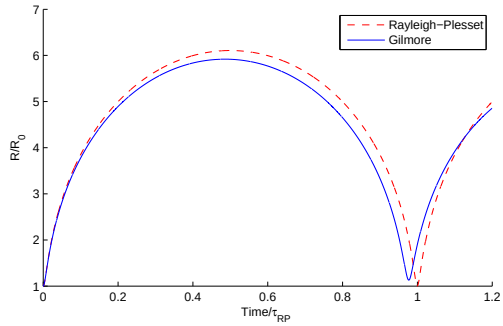

Figure 2: Comparison of predicted temporal variation of bubble radius from Rayleigh-Plesset and Gilmore equations for an initial pressure and radius of 100 bar and 0.01 m respectively. τ_{RP} is the collapse time for the Rayleigh–Plesset bubble.

much longer. The additional factors identified here have been modelled using the parameters of a scale model airgun; the initial bubble radius is taken as 0.014 m, the initial pressure is 100 bar and hydrostatic pressure is 1 bar. The numerical integration is performed using a fourth order Runge–Kutta method. To incorporate mass throttling and temperature effects, the ideal gas law pressure equation (5) is replaced by:

$$p = \frac{mR_G T}{V} + p_v \tag{7}$$

where m is the bubble gas mass, R_G is the gas constant, T is the bubble temperature and V is the bubble volume. When the gun is fired, the air expands through four 'ports' into the surrounding water. Depending on the gun design, the air may also pass through other internal constrictions before release. These orifices throttle the flow rate and considering the pressure differences involved, choked flow conditions can be assumed. The mass flow function is [16]:

$$\dot{m} = A\sqrt{\frac{p_G m_G}{V_G}\frac{2k}{k-1}\left[\left(\frac{p}{p_G}\right)^{\frac{2}{k}} - \left(\frac{p}{p_G}\right)^{\frac{k+1}{k}}\right]} \tag{8}$$

where p is limited to the sonic value, p_G^*:

$$p_G^* = p_G\left(\frac{2}{k+1}\right)^{\frac{k}{k-1}} \tag{9}$$

A is the orifice area, in this model taken as 336.9 cm^2, and the subscript G indicates the value inside the airgun chamber. The mass throttling limits the initial maximum radius, subsequently reducing the first period and the maximum bubble pressure achieved after the first collapse (figure 3).

The presence of the airgun body at the bubble centre has been identified as a contributing factor to the bubble dynamics [13]. The volume of air in the bubble is:

$$V = \frac{4}{3}\pi R^3 - V_{AG} \tag{10}$$

where V_{AG} is the volume of the airgun body, in this model taken as 6.54×10^{-5} m^3. This volume is then used to calculate the bubble pressure, which in effect is increased at the maximum bubble radius as compared with the bubble pressure where no body is present. The reduced pressure difference between the bubble and the water reduces the intensity and velocities of the collapse; therefore, the first bubble minimum is larger, and the following oscillations less intense (figure 3).

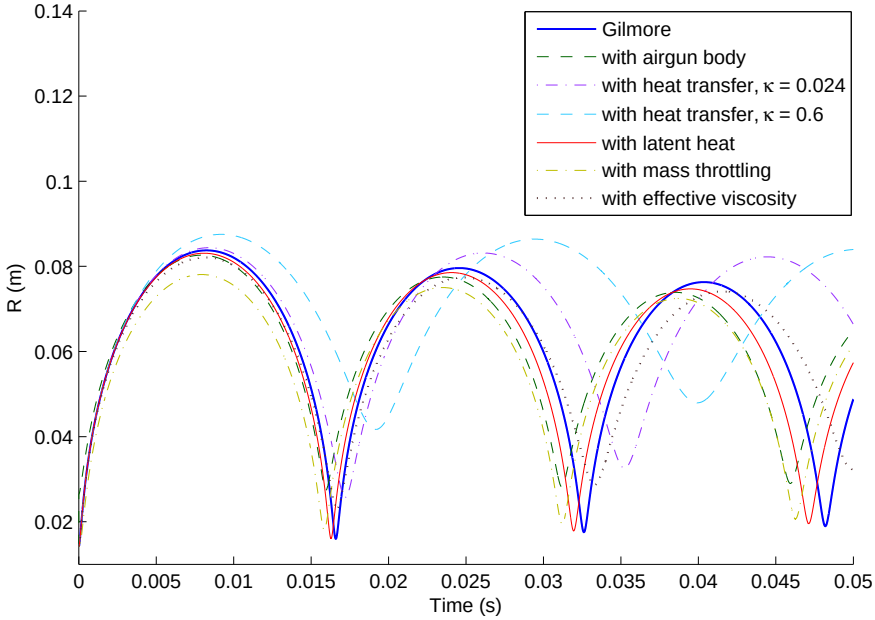

Figure 3: Effect on bubble radius of including different aspects to the Gilmore equation.

Laws et al. [9] include an effective viscosity, μ_{eff}, to account for turbulent motion at the bubble wall which occurs at large Reynolds numbers. This increases the heat transfer across the bubble wall and the viscous damping of the bubble oscillation.

$$\mu_{eff} = \mu(1 + KRe) \tag{11}$$

K is a constant, about 0.02. The Reynolds number, Re, is calculated based on the instantaneous bubble radius and velocity. The effect of increasing the viscosity has a small impact on the damping of the bubble (figure 3); note, when considered independently there is no heat transfer in the bubble, so this implementation only models the increased viscous damping.

Li et al [10] identified that Ziolkowski's [17] model (essentially Gilmore's model with k equal to 1.13) results in an equilibrium temperature well below that of the surrounding water. The inclusion of heat transfer in the model results in more realistic predictions of equilibrium temperatures. Laws et al. [9] give the thickness of the thermal boundary layer as:

$$d = 4DRe^{-\frac{3}{4}}Pr^{-\frac{1}{2}} \tag{12}$$

where D is the bubble diameter and Pr is the Prandtl number. The rate of heat conduction across this layer is:

$$\dot{Q} = \Delta T A \frac{\kappa}{d} \tag{13}$$

where ΔT is the difference in temperature across the bubble wall, A is the surface area of the bubble and κ is the thermal conductivity of the interface. Ni et al [11] studied a range of κ/d values from 2000 – 8000 W/m^{2}K and found correspondance with specific experimental data for a value of 4000 W/m^{2}K. Herring [6] states that the flow of heat outward is a function of the thermal conductivity of the gas. The thermal boundary layer will extend across the bubble interface, complicating the value of the thermal conductivity. Here, values for κ of 0.6 W/mK for water and 0.024 W/mK for air have been considered; d is updated through the calculations but is in the order of 100 µm. Due to turbulence, the area across which heat is conducted may be magnified — Laws et al. [9] used a factor of 10; however, in this example, the actual surface area is used. Modelling heat transfer lessens the drop in temperature as the bubble expands, allowing the bubble to reach a greater maximum radius. The temperature is also increased during collpase, which increases the pressure, arresting the collapse at a larger minimum radius. The magnitude of the following oscillations is likewise diminished (figure 3). The bubble temperature is shown in figure 4.

In place of classical heat transfer, Ziolkowski [18] proposed that the heat transfer takes place through latent heat released by evaporation and condensation at the bubble wall. Fujikawa and Akamatsu [4] produced a detailed mathematical formulation to consider these effects. Simpler models have been used by Laws et al. [9] and Cook et al. [1]. The vapour mass transfer is:

$$\dot{m}_v = \frac{\alpha_M A}{\sqrt{2\pi R_G}} \left[\frac{p_v^*}{\sqrt{T_w}} - \Gamma \frac{p_v}{\sqrt{T}} \right] \tag{14}$$

where α_M is the ratio of vapour molecules sticking to the phase interface and those impinging on it, about 0.04 [4], A is the surface area of the bubble, p_v^* is the equilibrium vapour pressure [4] and T_w is the temperature of the water. Γ is a correction factor, assumed to be 1 for these calculations. The heat flow due to the vapour mass transfer is given by:

$$\dot{Q} = \dot{m}_v L \tag{15}$$

where L is the latent heat of vaporization, taken as 2.45 J/kg. The impact on the bubble wall dynamics due to movement of the bubble wall as a result of mass flow has been ignored, as the additional terms are assumed negligible [1]. Only the effect on bubble temperature and pressure has been considered. Modelling the mass transfer due to evaporation and condensation has a small impact on the maximum radius and period of the bubble pulses (figure 3). The effect on the bubble temperature is also small (figure 4) and there is no appreciable difference to the final bubble temperature. Figure 5 presents the results of including all additional factors discussed here. Solutions have been calculated for both proposed limits of κ. Increasing the surface area in equation (13) would further increase the bubble period and damping.

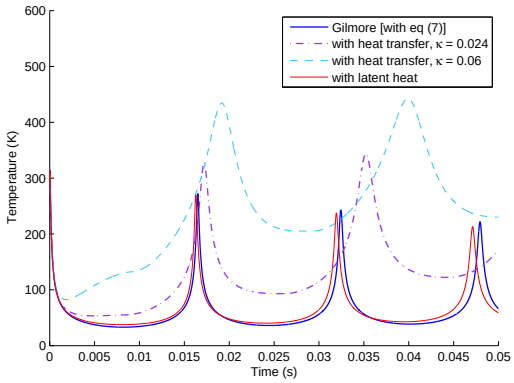

Figure 4: Effect on bubble temperature of including conductive heat transfer and heat transfer through latent heat.

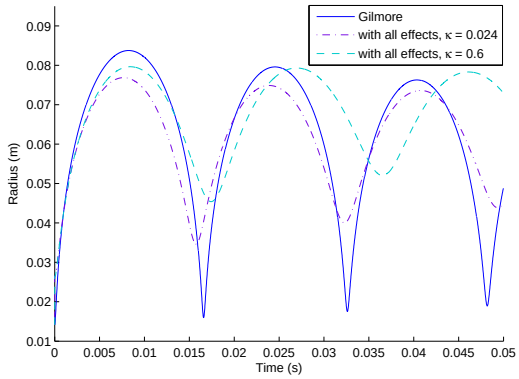

Figure 5: Combined effect on bubble radius of including all additional factors.

Conclusion

Various models have been studied that could account for differences in airgun bubble dynamics between theoretical predictions and experimental observations. From the above study, the most likely primary cause of additional damping to the seismic airgun bubble is heat transfer between the water and the air. This is potentially enhanced by an increase in bubble surface area due to turbulent motion near the bubble wall. Initial mass throttling as the air is released impacts the first maximum radius of the bubble significantly. The scale model parameters used in these numerical predictions may result in different emphasis on some factors when compared to predictions for a full scale airgun; these parameters have been chosen for comparison with experimental results. Further study will determine how the additional damping factors change with dimensional and pressure scaling.

Acknowledgements

This work has been funded by the Maritime Platforms Division of the Defence Science and Technology Organisation (DSTO) and the authors wish to acknowledge the support of Dr Stuart Cannon and Mr Warren Reid.

References

[1] Cook, J. A., Gleeson, A. M., Roberts, R. M. and Rogers, R. L., A spark-generated bubble model with semi-empirical mass transport, *Journal of the Acoustical Society of America*, **101**, 1997, 1908–1920.

[2] Dragoset, W., A comprehensive method for evaluating the design of airguns and airgun arrays, in *Offshore Technology Conference*, Houston, Texas, 1984, 75–84.

[3] Franc, J. and Michel, J., *Fundamentals of Cavitation*, Kluwer Academic Publishers, Dordrecht, The Netherlands, 2004.

[4] Fujikawa, S. and Akamatsu, T., Effects of the non-equilibrium condensation of vapour on the pressure wave produced by the collapse of a bubble in a liquid, *Journal of Fluid Mechanics*, **97**, 1980, 481–512.

[5] Gilmore, F., The growth or collapse of a spherical bubble in a viscous compressible liquid, Technical Report Report No. 26-4, California Institute of Technology, 1952.

[6] Herring, C., Theory of the pulsations of the gas bubble produced by an underwater explosion, in *Underwater Explosion Research: v. 2, 1950*, Officer of Naval Research, Dept of the Navy, 1949.

[7] Johnston, R. C., Development of more efficient airgun arrays: Theory and experiment, *Geophysical Prospecting*, **30**, 1982, 752–773.

[8] Langhammer, J. and Landro, M., Temperature effects on airgun signatures, *Geophysical Prospecting*, **41**, 1993, 737–750.

[9] Laws, R. M., Hatton, L. and Haartsen, M., Computer modelling of clustered airguns, *First Break*, **8**, 1990, 331–338.

[10] Li, G. F., Cao, M. Q., Chen, H. L. and Ni, C. Z., Modeling air gun signatures in marine seismic exploration considering multiple physical factors, *Applied Geophysics*, **7**, 2010, 158–165.

[11] Ni, C. Z., Chen, H. L., Liu, J., Ye, Y., Niu, H., Cao, M. Q. and Liu, Y., Parameter optimization in air-gun type-dependent signature modelling, in *73rd EAGE Conference & Exhibition incorporating SPE EUROPEC*, Vienna, Austria, 2011.

[12] Safar, M. H., Efficient design of airgun arrays, *Geophysical Prospecting*, **24**, 1976, 773–787.

[13] Schulze-Gattermann, R., Physical aspects of the airpulser as a seismic energy source, *Geophysical Prospecting*, **20**, 1972, 155–192.

[14] Vaage, S. and Ursin, B., Computation of signatures of linear airgun arrays, *Geophysical Prospecting*, **35**, 1987, 281–287.

[15] Vokurka, K., Comparison of rayleigh's, herring's and gilmore's models of gas bubbles, *Acustica*, **59**, 1986, 214–219.

[16] White, F., *Fluid Mechanics, 5th Edition*, McGraw Hill, New York, NY, 2003.

[17] Ziolkowski, A., A method for calculating the output pressure waveform from an airgun, *Geophysical Journal of the Royal Astronomical Society*, **21**, 1970, 137–161.

[18] Ziolkowski, A., An airgun model which includes heat-transfer and bubble interactions, in *SEG Annual Meeting*, Dallas, Texas, 1982, 187–189.